Turkish Journal of Physics

http://journals.tubitak.gov.tr/physics/

Research Article

Turk J Phys
(2014) 38: 165 – 173

doi:10.3906/fiz-1310-8

Fast numerical algorithm for a high-precision 6D electromagnetic positioning navigation system

Qian XIANG[1,2,*], **Shiqing WANG**[1,2], **Haifeng LIU**[1]
[1]Southwestern Institute of Physics, Chengdu, P.R. China
[2]Institute of Nuclear Engineering and Technology, The Engineering & Technical College of Chengdu University of Technology, Leshan, P.R. China

Received: 29.10.2013 • **Accepted:** 24.03.2014 • **Published Online:** 11.06.2014 • **Printed:** 10.07.2014

Abstract: A fast numerical algorithm is proposed for the 6 degrees of freedom electromagnetic navigation system, which can be used to improve surgical operations guided by medical images. Both the rotation transformation technique and optimization technique are adopted in the algorithm. The results from simulations show that the calculating time is improved greatly under the required precision in the surgery. A navigation system based on the algorithm can make the medical device's dimensions miniaturized and the structure simplified and portable. The performance and application scope of the electromagnetic positioning navigation system can be improved.

Key words: Six degrees of freedom, electromagnetic positioning navigation, numerical algorithm

1. Introduction

As a relatively advanced space positioning technology, the electromagnetic positioning navigation technology may achieve 3-dimensional positioning. The property of the electromagnetic field penetrating into the human body can used to position surgical tools inside the body. The tools can be operated by a robot during surgery guided by medical images. This work has attracted increasing attention from experts and various scientific research institutions in China and worldwide [1–3].

The electromagnetic positioning navigation system is composed of a waveform generating and control circuit, a power amplifier, a transmitting coil, an exploring coil (probe), a detection circuit, a subsequent controller, etc. The time-sharing electromagnetic field is transmitted into a space of interest from a set of transmitting coils. The probes receive the field and produce the position and orientation in 5 degrees of freedom (5D) or 6 degrees of freedom (6D) inside the human body based on the results from the probes. Then the navigation can decide the further operation. The research on the electromagnetic navigation technology dates from the 1950s or the 1960s. At present quite a number of patent technologies [4,5] have been harvested.

However, this technology developed relatively late in China and the research on such a technology was performed mainly theoretically in the past. In recent years, the electromagnetic navigation technology has developed very fast in the medical treatment field. In the theoretical research, the typical investigation is the tetrahedral differential dipole endoscope positioning technology jointly developed by Fuzhou University and Fujian Medical University, which realizes the miniaturization of the endoscope probe. However, this technology mainly focuses [6–8] on the 5D navigation of the probe, with slow research progress and without

*Correspondence: xiangqian1000@163.com

further research into the whole system. In consideration of the application of the electromagnetic navigation system, the researchers should concentrate on, during the R&D process, the miniaturization of the system dimensions, the simplification of the structure, and the precision of the positioning navigation. For the existing problems [9–15] of the electromagnetic positioning navigation system, from the view of the system design, the electromagnetic field is recalculated and the analogue simulation is conducted to optimize the structure of the transmitting coils and the detecting probe so as to materialize the precise positioning navigation of the 6D probe.

2. Fundamentals of electromagnetic navigation

As shown in Figure 1, the center of the circumferential coil current is placed at the origin of the Cartesian system of coordinates and the vector of magnetic induction, B, can be gained based on the Biot–Savart law at an arbitrary point P $(x,\ y,\ z)$ in the system:

$$B = \sum_{i=1}^{n} B_i = \sum_{i=1}^{n} \frac{\mu_0 I_0 \sin(\omega t) l_i}{4\pi} \times \frac{r}{|r|^3} \tag{1}$$

In the equation, B_i is the magnetic induction generated by the ith current element of the circumferential coil at the investigation point P, μ_0 the permeability of vacuum, Il_i the ith current element of the circumferential coil, and r the vector pointing to the investigation point from the circumferential current.

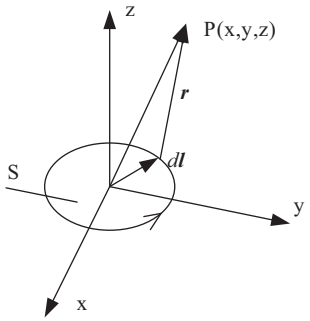

Figure 1. A circumferential coil current with the center at origin of coordinates.

When the current loop with a radius of a lies in the x–y plane, the center of the circle coincides with the origin and the normal of the current loop in the axis z. The 3 magnetic induction components of B, (B_x, B_y, B_z), at a certain point P in the space can be expressed as follows [4]:

$$B_x = \frac{\lambda\mu_0 I}{2\pi} \frac{xz}{(x^2+y^2)\sqrt{\left(a+\sqrt{(x^2+y^2)}\right)^2+z^2}} \left(-K(\alpha) + E(\alpha)a^2 + x^2 + y^2 + \frac{z^2}{\left(a-\sqrt{(x^2+y^2)}\right)^2+z^2} \right) \tag{2}$$

$$B_y = \frac{\lambda\mu_0 I}{2\pi} \frac{yz}{(x^2+y^2)\sqrt{\left(a+\sqrt{(x^2+y^2)}\right)^2+z^2}} \left(-K(\alpha) + E(\alpha)a^2 + x^2 + y^2 + \frac{z^2}{\left(a-\sqrt{(x^2+y^2)}\right)^2+z^2} \right) \tag{3}$$

$$B_z = \frac{\lambda\mu_0 I}{2\pi} \frac{1}{\sqrt{\left(a+\sqrt{(x^2+y^2)}\right)^2+z^2}} \left(K(\alpha) + E(\alpha)a^2 - x^2 - y^2 - \frac{z^2}{\left(a-\sqrt{(x^2+y^2)}\right)^2+z^2} \right) \tag{4}$$

In the equation:

$$K(\alpha) = \int_0^{\frac{R}{2}} \frac{d\theta}{\sqrt{(1-\alpha^2\sin^2\theta)}} \tag{5}$$

$$E(\alpha) = \int_0^{\frac{R}{2}} \sqrt{\left(1-\alpha^2\sin^2\theta\right)} d\theta \tag{6}$$

$$\alpha = \sqrt{\frac{4ar}{(a+r)^2+z^2}} \tag{7}$$

The induced electromotive force is governed by Faraday's law of electromagnetic induction. If an exploring coil with the number of windings, N, and the sectional area, S_p, is placed at P $(x,\ y,\ z)$, we obtain an equation for ε:

$$\varepsilon = -N_p \frac{d\left[(B_x i + B_y j + B_z k)\cdot S_p \cdot (\cos\alpha_p i + \cos\beta_p j + \cos\gamma_p k)\right]}{dt} \tag{8}$$

where ε is the induced voltage (generated by the exploring coil), N_p is the number of windings of the exploring coil, and $\cos\alpha_p$, $\cos\beta_p$, and $\cos\gamma_p$ are the cosines of the attitude angle of the exploring coil, respectively. Now the problem is that when the position and the attitude angle of the transmitting coil are known, it is impossible to find out the position (x_p, y_p, z_p) and the attitude angle $(\alpha_p, \beta_p, \gamma_p = f(\alpha_p, \beta_p))$ of the exploring coil by using the only one equation (8). Here are 6 parameters (5 independent parameters actually). To obtain the position and the orientation of the probe, a group of transmitting coils in a certain structure must be designed. Therefore, the equations are set up. To make sure the system is solved, the number of transmitting coils must be larger than 5. The exploring coil can establish the relationship among the transmitting coils.

Furthermore, the system modeling and its algorithm are studied carefully. Some new methods and techniques are adopted in this research paper. Firstly, the technique of rotation transformation of the quaternion makes the modeling of the electromagnetic radiation system more convenient. Secondly, some optimization techniques are employed to assure both the positioning precision and the computed speed of the algorithm. Therefore, in this paper the adopted techniques in algorithm are given as follows.

3. Numerical algorithm of electromagnetic navigation

The magnetic induction at the investigation point P will be measured with the small coil ring shown in Figure 2:

$$B = \int dB = \int \frac{\mu_0 I_0 \sin(\omega t) dl}{4\pi} \times \frac{r}{|r|^3} \tag{9}$$

In Eq. (9), the position vector, r, is

$$r = r_p - r' = (x_p - x)\, i + (y_p - y)\, j + (z_p - z)\, k \tag{10}$$

where r_p is the distance vector from the origin of coordinates to the center of the exploring coil, r the distance vector from the origin of coordinates to the current element of the transmitting coils, (x_p, y_p, z_p) the coordinates of the exploring coil, and (x, y, z) the coordinates of the current element of the transmitting coils, respectively.

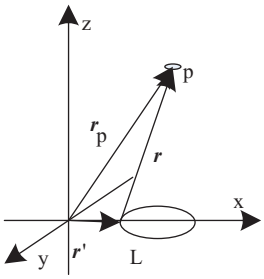

Figure 2. A circumferential coil with center not at origin of coordinates.

Based on Faraday's law of electromagnetic induction, the induced voltage, ε_p, can be described as:

$$\varepsilon_p = -N_p \frac{d(B \cdot S_p)}{dt} = -\frac{N_p N \omega \mu_0 \pi a^2 I_0 \cos \omega t a_p^2}{4r^5} [3(n \cdot r)r - r^2 n] \cdot n_p \tag{11}$$

In Eq. (11), N and N_p are the numbers of windings of the transmitting coil and the exploring coil respectively, a and a_p the radius of the transmitting coil and the exploring coil respectively, n the orientation of the transmitting coil, and n_p the orientation of the exploring coil. Similarly, the position (x_p, y_p, z_p) and the attitude $(\alpha_p, \beta_p, \gamma_p = f(\alpha_p, \beta_p))$ of the exploring coil are examined. To find out the parameters, it is required that at least 5 transmitting coils are in a certain structure. The electromagnetic field is transmitted in turn under the control of the sequential circuit. The configuration of the transmitted coils is defined in the way the original coil is rotated to the position with rotation matrices. In this paper, the rotation matrix by using the quaternion algorithm rather than the Euler angle transformation is found, shown in Figure 3.

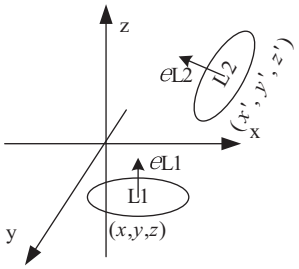

Figure 3. Two circumferential coils in a rectangular coordinate system.

Let the coil L1 be the benchmark. The central coordinate $\left(x', y', z'\right)$ of the coil L2 is gained through the translation of the central coordinate (x, y, z) of the coil L1. The orientation e_{L2} of the coil L2 is received through the orientation e_{L1} of the coil L1 rotating for θ degrees around a certain axis. The rotation matrix is as follows:

$$Q = \begin{vmatrix} w^2 + X^2 - Y^2 - Z^2 & 2XY - 2Zw & 2XZ + 2Yw \\ 2XY + 2Zw & w^2 + Y^2 - X^2 - Z^2 & 2YZ - 2Xw \\ 2XZ - 2Yw & 2YZ + 2Xw & w^2 + Z^2 - Y^2 - X^2 \end{vmatrix} \tag{12}$$

$$\begin{vmatrix} X \\ Y \\ Z \end{vmatrix} = \begin{vmatrix} V_x \\ V_y \\ V_z \end{vmatrix} \sin\frac{\theta}{2} \tag{13}$$

In Eqs. (12) and (13), $w = \cos\frac{\theta}{2}$, V_x, V_y, and V_z represent the projection on the axis x, y, and z respectively of the unit vector rotating around the certain axis. Compared with the Euler transformation, the quaternion will be more efficient and there is no singularity.

The exploring coil may be more than one. One exploring coil can only form a 5D navigation system. It cannot form a complete subcoordinate system. Obviously some information on the orientation of the probe is missing. This limits greatly the application of the electromagnetic navigation system in the medical field. However, a probe with 2 unparallel exploring coils can solve the difficulty and form a complete coordinate system. This kind of probe makes the surgical tool move in the correct way.

For an easy analysis of the detector model, the detecting probe will consist of 2 mutually nonparallel coils at different positions. Thus sub-Cartesian coordinates, x', y', and z', can be also defined inside the probe as shown in Figure 4. The relation between the real coordinate system and the subcoordinate system can be seen in Figure 4. The translations to the midpoint p of the central coil p1 of the probe are x', y', and z' and the orientation to the real coordinate is determined by the orientations n_1 and n_2 of the 2 orthogonal exploring coils. Let the axis z' be parallel to orientation, n_1, of the one coil. Then the axis y' is determined by $n_{y'} = n_1 \times n_2$ and the axis x' by $n_{x'} = -n_1 \times n_{y'}$. Again, when the probe rotates, the exploring system will rotate relatively to the benchmark status. The position of the probe top can be gained through change in the coordinates of the exploring coil's central position. Therefore, this 6D positioning will give current information of the position and the orientation of the probe.

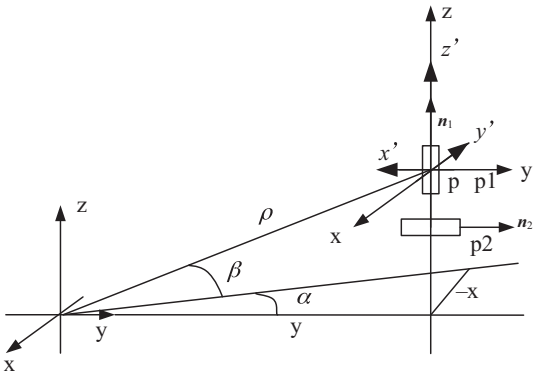

Figure 4. Relationship between transmitting coordinate system and exploring coordinate system.

4. Electromagnetic navigation model

On the basis of the theoretical analysis mentioned above, a 6D electromagnetic positioning navigation system model is designed as shown in Figure 5. Three sets of 2 orthogonal transmitting coils are placed in the transmitting coordinate system XYZ, with the transmitting coil 1 and 2, 3 and 4, and 5 and 6 forming a set of orthogonality respectively. Two unparallel exploring coils are set as a probe.

As shown in Figure 6, the exploring coils in the probe will gain a set of induced voltages, which determine the translation and the orientation of the subcoordinates system. The magnetic fields generated by the time-sharing transmitting of 6 position-fixed transmitting coils are mutually independent. Twelve induced voltages of the probe, ε_{ip}, can be expressed as follows:

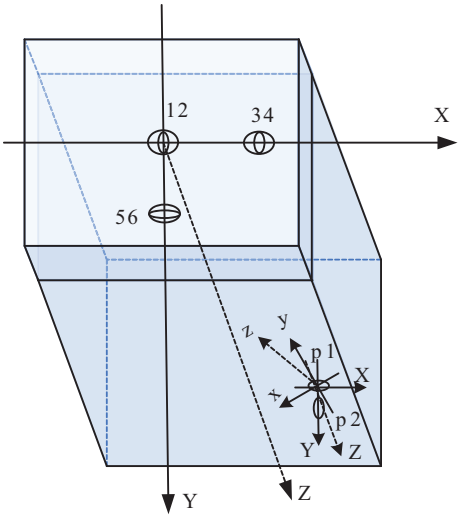

Figure 5. A electromagnetic positioning navigation model with three sets of two orthogonal circumferential coils.

$$\varepsilon_{ip} = -\frac{N_p N \omega \mu_0 \pi a_i^2 I a_p^2}{4 r_i^5} [3(n_i \cdot r_i) r_i - r_i^2 n_i] \cdot n_p \tag{14}$$

Eq. (14) can be rewritten as

$$\varepsilon_{ip} = -\lambda_i n_p \cdot [(M_i (x_p - x_i) - Q_{i1})\, i + (M_i (y_p - y_i) - Q_{i2})\, j + (M_i (z_p - z_i) - Q_{i3})\, k] \tag{15}$$

$$M_i = 3\cos\alpha_i (x_p - x_i) + 3\cos\beta_i (y_p - y_i) + 3\cos\gamma_i (z_p - z_i) \tag{16}$$

$$Q_{i1} = r_i^2 \cos\alpha_i; Q_{i2} = r_i^2 \cos\beta_i; Q_{i3} = r_i^2 \cos\gamma_i \tag{17}$$

In Eqs. (14)–(17), i is changed from 1 to 6, transmitting coil (s), and p= 1, 2 exploring coil (s). The system composed of 12 equations is complete space. The target information of the 2 positions $(x_p, y_p, z_p, \alpha, \beta, \gamma)$ can be determined. In the context of Visual Studio 2008, the simulation experiment has been implemented for the magnetic field constructed by the model. The precise start point of the measuring space's coil has been found successfully.

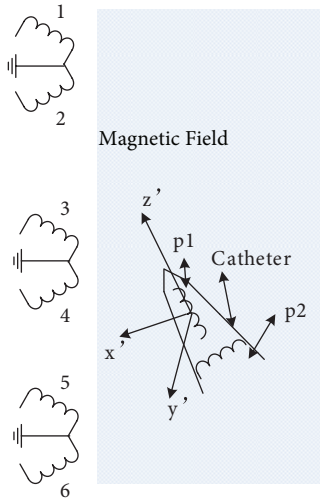

Figure 6. Model for measurement.

The above-mentioned orientation and position information of the exploring coils are obtained under the ideal condition. Practically, errors in the measurement come from a number of factors, such as the fabrication process, the exciting current, and the temperature. The theoretical detecting voltage signal ε_{ip} is not equal to the actual one v_{ip} exactly, namely

$$v_{ip} - \varepsilon_{ip} = \xi_i \tag{18}$$

ξ_i is the error voltage. The solution of this over-determined system must ensure $\xi_i^2 = \min \sum_{i=1}^{n} [v_{ip} - \varepsilon_{ip}]^2$, in which n is the coil number. The position and attitude $(x_p, y_p, z_p, \alpha_p, \beta_p, \gamma_p)$ of each exploring coil can be solved precisely. In this paper the Gauss–Newton method is employed in the fast algorithm and it converges faster [16–19]. It is not only conducive to the reduction of iteration delay and data processing time, but also improves the precision of the electromagnetic positioning navigation and realizes the miniaturization of the probe.

5. Simulation and discussion

To verify the algorithm's performance, the magnetic field distribution of the solenoid in a space (in a region measuring 500 mm × 500 mm × 500 mm) was computed using Visual Studio 2008. Three different types of algorithms were compared with each other, i.e. the strict algorithm, the current-loop approximation algorithm, and the new fast numerical algorithm. The results with the 3 different algorithms are indicated by the red, green, and blue lines, respectively. The system uses Cartesian coordinates. The effective space of the x-coordinate ranges from –250 mm to 250 mm and that of the y-coordinate ranges from –250 mm to 250 mm, while that of the z-coordinate ranges from 50 mm to 550 mm. The 3-dimensional magnetic field distributions of the 3 algorithms when the solenoid was placed at (0, 0, 0) are shown in Figure 7. Their normalized computing time ratio was 10^6:70:1. Figure 8 shows a comparison of each magnetic induction component using the 3 algorithms.

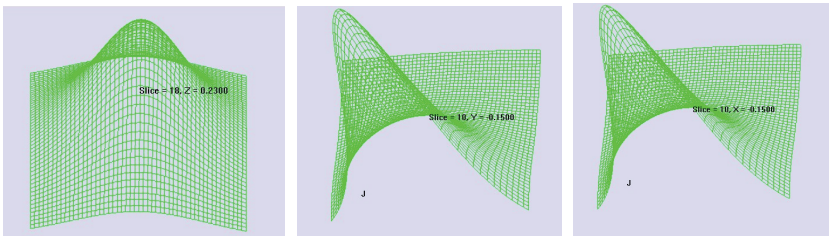

(a) XY Plane (b) XZ Plane (c) YZ Plane

Figure 7. Spatial distributions of magnetic induction.

As shown in Figure 8, the result obtained using the current-loop approximation algorithm is exactly the same as the one with the fast numerical algorithm. However, the magnetic induction component in parts of the space deviates from the result computed using the strict algorithm to a certain degree, shown a, b, and c in Figure 8. These deviations will directly affect the precision of positioning in the area of interest.

The result obtained by using the strict algorithm is very precise, but the computation is time-consuming and highly intensive, which means the practical requirement of the application is hardly satisfied. For real-time positioning in high-precision surgery, an optimization is necessary on the structure of the solenoid coil, the magnetic field exciting current, the system structure, and other features to eliminate the deviation caused by the finite length effect of the solenoid coil effectively. The new algorithm greatly improves the computational speed and it satisfies the requirements in terms of spatial precision ($<$1 mm), spatial orientation ($< 1^\circ$), and high-precision real-time positioning.

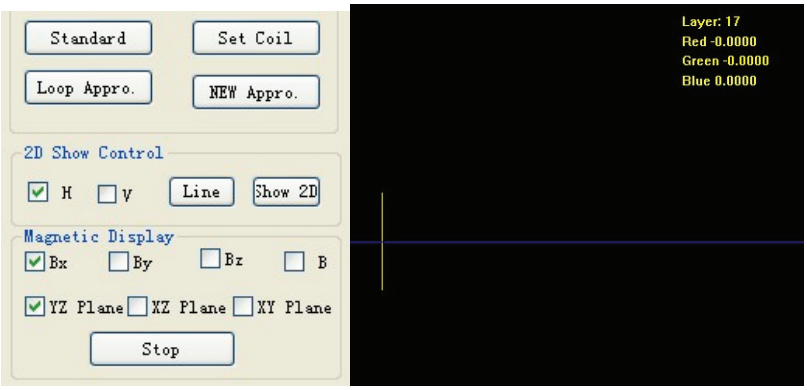

(a) YZ plane showing B_x

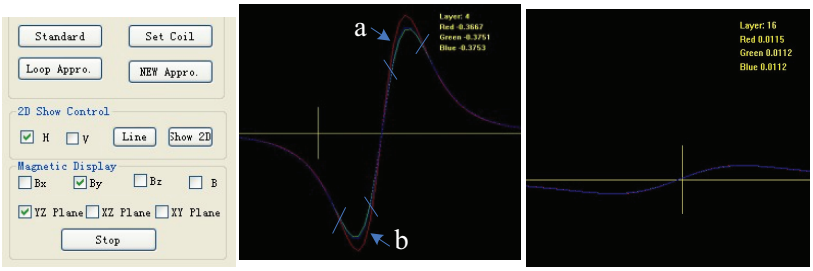

(b) YZ plane showing B_y

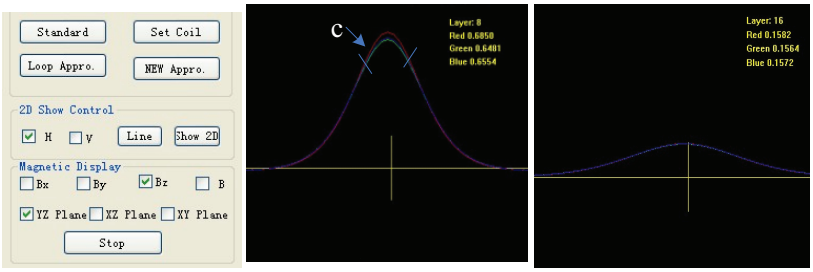

(c) YZ plane showing B_z

Figure 8. Magnetic induction component of the 3 algorithms.

6. Conclusion

A fast numerical algorithm is discussed for the electromagnetic navigation system in this paper. A model based on the algorithm meets the requirement of real-time surgical operations guided by medical images and provides a method to build the electromagnetic navigation system. The results from the simulations show that the rotation matrix adopting the quaternion algorithm and the optimization of the structure of the transmitted coils are not only more effective, but also eliminate the effect of the limited length of the solenoid coil effectively. An instrument design and construction based on this powerful algorithm is in the works. These techniques will make the system structure miniaturized and more portable. It will improve surgery guided by medical images.

Acknowledgments

Thanks to my colleagues' efforts on the study. The work was supported by the Science and Technology Bureau of Leshan, China (NO.2013GZD042), and Science and Technology Research Project, Ministry of Education, Sichuan, China (NO.12ZB194).

References

[1] Baldoni, J. A.; Yellen, B. B. *IEEE Trans. Magn.* **2007**, *43*, 2430–2432.

[2] Hu, C.; Meng, M. Q. H.; Mandal, M. *Int. J. Inform. Acquisition* **2005**, *2*, 23–36.

[3] Andra, W.; Danan, H.; Kirmssw, W.; Kramer, H. H.; Saupe, P.; Schmieg, R.; Bellemann, M. E. *Phys. Med. Biol.* **2000**, *45*, 3081–3093.

[4] Schneider, *U.S. Patent No. 6073043*, **2000**.

[5] Anderson, *U.S. Patent No. 7158754*, **2007**.

[6] Nolte, L. P.; Beutler, T. *Injury* **2004**, *35*, 6–16.

[7] Nijmeh, A.D.; Goodger, N.M.; Hawkes, D. *Brit. J. Oral Max. Surg.* **2005**, *43*, 294–302.

[8] Paperno, E. *IEEE Trans. Magn.* **2001**, *37*, 1938–1940.

[9] Lavallee, S.; Szeliski, R. *IEEE Trans. Pattern Anal. Mach. Intell.* **1995**, *17*, 378–390.

[10] McFee, J.; Das, Y. *IEEE T. Antenn. Propag.* **1981**, *29*, 282–287.

[11] Baluja, S.; Simon, D. *Appl. Intell.* **1998**, *8*, 7–19.

[12] Birkfellner, W.; Watzinger, F.; Wanschitz, F. *IEEE Trans. Med. Imaging.* **1998**, *17*, 737–742.

[13] Nara, T.; Suzuki, S. *IEEE Trans. Magn.* **2006**, *42*, 3291–3293.

[14] Tian, H. Q.; Wu, D. M.; Wang, J. H.; Du, Z. J.; Sun, L. N. *Robot.* **2011**, *33*, 59–65.

[15] Shi, X. Z.; Hu, C.; Xiang, W. H.; Song, S.; Wang, X. J. *Chinese Journal of Sensors and Actuators* **2011**, *24*, 1569–1573.

[16] Hu, C.; Meng, M. Q. H.; Mandal, M. *IEEE Trans. Magn.* **2007**, *43*, 4096–4101.

[17] Yang, W. A.; Hu, C.; Li, M.; Meng, M. Q. H.; Song, S. *IEEE Trans. Magn.* **2010**, *46*, 4023–4029.

[18] Hu, C.; Li, M.; Song, S.; Yang, W. A.; Zhang, R.; Meng, M. Q. H. *IEEE Sensors J.* **2010**, *10*, 903–913.

[19] Yang, W. A.; Hu, C.; Meng, M. Q. H.; Song, S.; Dai, H. D. *IEEE Trans. Magn.* **2009**, *45*, 3092–3099.